TRR
JOURNAL OF THE TRANSPORTATION RESEARCH BOARD

Research Article

Transportation Research Record
1–12

DOI: 10.1177/0361198120974677
journals.sagepub.com/home/trr
SAGE

Train Scheduling Method to Reduce Substation Energy Consumption and Peak Power of Metro Transit Systems

Bo Jin[1], Xiaoyun Feng[1], Qingyuan Wang[1], Pengfei Sun[1], and Qian Fang[1]

Abstract

The rapid development of metro transit systems brings very significant energy consumption, and the high service frequency of metro trains increases the peak power requirement, which affects the operation of systems. Train scheduling optimization is an effective method to reduce energy consumption and substation peak power by adjusting timetable parameters. This paper proposes a train timetable optimization model to coordinate the operation of trains. The overlap time between accelerating and braking phases is maximized to improve the utilization of regenerative braking energy (RBE). Meanwhile, the overlap time between accelerating phases is minimized to reduce the substation peak power. In addition, the timetable optimization model is rebuilt into a mixed integer linear programming model by introducing logical and auxiliary variables, which can be solved by related solvers effectively. Case studies based on one of Guangzhou Metro Lines indicate that, for all-day operation, the utilization of RBE would likely be improved on the order of 23%, the substation energy consumption would likely be reduced on the order of 14%, and the duration of substation peak power would likely be reduced on the order of 66%.

Metro transit systems have been developing rapidly in recent years because of their convenience and large transport capacity. As a result of increasing energy prices and environmental issues, the very significant energy consumption of metro transit systems has become a non-negligible challenge. Energy conservation in metro transit systems has become a research topic (*1*). The energy consumption of metro transit systems can be divided into two parts: non-traction energy consumption and substation energy consumption. Non-traction energy consumption refers to the energy required to keep stations, depots, and other facilities running, which is supported by the non-traction supply. Substation energy consumption reflects the power required to operate the trains running on systems, and is supported by the traction substations (*2*). The substation energy consumption accounts for around 50% of the total energy consumption of systems (*3*). Thus, reducing substation energy consumption is an effective approach to reduce the energy consumption of metro transit systems. Energy-efficient train scheduling and control are effective measures to reduce substation energy consumption (*4*), therefore, train dispatchers and drivers, respectively, must pay attention to these two aspects.

Most studies of energy-effective train control focus on the optimization of speed profiles to minimize motion resistance. The speed profile optimization problem is to find the best driving strategy considering the train data, line data, and operation constraints. The Scheduling and Control Group of South Australia conducts studies of speed profile optimization based on Pontryagin's Maximum Principle. Speed limits (*5*) and varying gradients (*6*) are introduced into the speed profile optimization problem. Jin et al. transformed the speed profile optimization problem into a mixed integer linear programming (MILP) model and solved it by CPLEX solver (*7*). However, these studies ignore the utilization of regenerative braking energy (RBE), which recovers 33% of the total traction energy (*1*).

The regenerative braking technique has been widely applied in metro transit systems (*3*). For a train with electric traction motors, the motors can be used as

[1]School of Electrical Engineering, Southwest Jiaotong University, Chengdu, China

Corresponding Author:
Pengfei Sun, spf0325@163.com

Table 1. Literature on Energy-Efficient Train Scheduling Based on Overlap Time

Literature	Overlap time category	Method
Ramos et al. (*16*)	t_{ab}	Mixed integer programming
Yang et al. (*17*)	t_{ab}	Genetic algorithm
Ning et al. (*18*)	t_{ab}	Genetic algorithm
Zhao et al. (*19*)	t_{ab}	Simulated annealing algorithm
This paper	$t_{aa} + t_{ab}$	Mixed integer linear programming

Note: t_{ab} = overlap time between accelerating and braking phases; t_{aa} = overlap time between accelerating phases.

generators when braking. The generated RBE can be fed back into the overhead contact line or the third rail, which can be utilized by accelerating trains running in the same substation section. However, if there is no accelerating train when RBE is produced, then it will be wasted through thermal resistance. Many strategies and technologies are proposed to improve the utilization of RBE to reduce substation energy consumption (*8*). Energy storage devices are applied in metro transit systems to save RBE and manage it (*9*). Nevertheless, because of their limited capacity and high cost, energy storage devices are not widely applied in the real world (*3*). Most of the studies focus on coordinating the operation of trains to make different trains accelerate and brake at the same time, aiming to improve the utilization of RBE. Optimizing speed profiles is one of the methods to coordinate the operation of trains. Sun et al. added an accelerating regime into the speed profile when RBE was available (*10*). The simulation results showed that the proposed method can utilize RBE efficiently. However, the optimization of speed profiles without timetable changes limits the adjustable space for coordination.

Energy-efficient train scheduling is another effective method to improve the utilization of RBE by adjusting timetable parameters (e.g., headway, running times and dwell times). Liu et al. analyzed the relationship between headway and the utilization of RBE (*11*). The simulations showed that there was an optimal value maximizing the utilization rate. Su et al. developed a cooperative train control model to adjust the departure times of accelerating trains, to utilize the RBE from braking trains (*12*). Liu et al. designed an improved artificial bee colony algorithm to solve the cooperative control model, in which headway and dwell times were optimized to coordinate the accelerating and braking trains running in the same substation section (*13*). Wang et al. proposed an energy-efficient train operation approach by integrating train scheduling and train control (*14*). An integrated model was built based on a space–time network, which was solved by dynamic programming. In addition, Albrecht considered reducing the peak power into the cooperative control model, in which running times were adjusted to synchronize the accelerating and braking phases (*15*). To simplify the cooperative control model, the overlap time between accelerating and braking phases is proposed to measure the utilization of RBE (*16*). Then, the coordination of accelerating and braking trains is realized by maximizing the overlap time (*17–19*). More related to the present paper, Yang et al. built an integer programming model to maximize the overlap time by adjusting headway and dwell times (*17*). However, only the overlap time between two successive trains was considered. Ning et al. considered the overlap time of multiple trains running in the same substation section to improve the utilization of RBE (*18*). Zhao et al. proposed a two-objective optimization model, taking into account the passenger waiting time and the utilization of RBE to optimize the timetable (*19*). The utilization of RBE was improved by overlapping the accelerating and braking phases. When multiple trains depart from stations simultaneously, the peak power of a metro transit system can be very large, which will affect the operation of the system (*20*). The peak power can be reduced by desynchronizing the departure of trains, which is not considered in the studies based on the overlap time. Table 1 gives a comparison between studies based on the overlap time and the present paper.

The main contribution of this paper can be given as follows.

(1) The overlap time between accelerating phases (t_{aa}) is first proposed in this paper, and its calculation method is elaborated. In addition, a train timetable scheduling model considering the optimization of t_{aa} is built, in which t_{aa} is minimized to reduce the substation peak power.
(2) The calculation formulas of t_{aa} and t_{ab} are linearized by introducing logical and auxiliary variables. Then the train timetable scheduling optimization model is rebuilt into a MILP model, which can be solved by existing solvers to get the optimal solution.

The rest of the paper is organized as follows: Coordinating the operation of trains by overlapping accelerating and braking phases is introduced in the next

section. The MILP model of timetable optimization is then built. Simulations based on one of Guangzhou Metro Lines are then presented. Finally, a brief discussion and conclusion are given.

Problem Statement

Notations

For a better understanding of this paper, the notations are introduced as follows.

Symbols

K: number of operating trains in time interval $[T_s\ T_e]$;
$2N$: number of stations belonging to the substation, $\{1,2,\ldots,N\}$ for the up direction, $\{N+1,\ N+2,\ldots,\ 2N\}$ for the down direction;
m, n: train indices, $m, n \in \{1,2,\ldots,K\}$;
i, j: symbol of station, $i, j \in \{1,2,\ldots,2N-1\}$.

Parameters

t: train running time;
$[T_s\ T_e]$: optimized time period;
t_{aa}: overlap time between accelerating phases;
t_{ab}: overlap time between accelerating and braking phases;
E_{sub}: total substation energy consumption;
E_{urbe}: total unutilized regenerative braking energy;
E_{arbe}: total available regenerative braking energy;
P_{sub}: substation power;
P_p: substation peak power;
P_n: substation power of train n;
η: utilization rate of regenerative braking energy;
$t_{a,n,i}$: duration of the accelerating phase of train n from station i to station $i+1$;
$t_{b,n,i}$: duration of the braking phase of train n from station i to station $i+1$;
$R_{n,i}$: running time of train n from station i to station $i+1$;
T_s: minimum safe headway;
$W_{n,i}$: dwell time of train n at station i;
$\boldsymbol{\delta}$: matrix of logical variable δ;
$\boldsymbol{\alpha}$: matrix of auxiliary variable α;
$\boldsymbol{\eta}$: matrix of logical variable η;
$\boldsymbol{\beta}$: matrix of auxiliary variable β;
$\boldsymbol{D}$: matrix of decision variable $D_{n,i}$;
$\boldsymbol{A}$: matrix of decision variable $A_{n,i}$;
$\boldsymbol{X}$: decision variable matrix of MILP;
$\boldsymbol{F}$: objective function coefficient matrix of MILP;
$\boldsymbol{M}_1$, $\boldsymbol{m}_1$: inequality constraints coefficient matrices of MILP;
$\boldsymbol{M}_2$, $\boldsymbol{m}_2$: equality constraints coefficient matrices of MILP;
w_{aa}, w_{ab}: weight parameters of t_{aa} and t_{ab}.

Logical and Auxiliary Variables

δ: logical variable to distinguish the relationship between departure times;
α: auxiliary variable to replace the product of logical variable δ and decision variable;
η: logical variable to distinguish the relationship between departure time and arrival time;
β: auxiliary variable to replace the product of logical variable η and decision variable.

Decision Variables

$D_{n,i}$: departure time of train n at station i;
$A_{n,i}$: arrival time of train n at station i.

Model Assumption

Accounting for the operation characteristics of metro transit systems, assumptions are formulated as follows.

(1) When the running time is given, the train control strategy of this section is fixed. Time lengths of accelerating and braking phases are constant, and can be calculated based on the control strategy.
(2) The RBE can be utilized by accelerating trains operating in the same substation section. Otherwise, it will be wasted via a thermal resistor. Energy storage technology is not considered.
(3) The substation power is simplified as the sum of the power of multiple trains running in this substation section. Transmission losses of energy and auxiliary power consumption are assumed to be constant.
(4) Improving the utilization of RBE by overlapping braking and cruising phases is not considered in this paper, because the effect is not obvious compared with overlapping braking and accelerating phases. Although trains in cruising phases can also be drawing energy and could benefit the better utilization of RBE, the major consumers of RBE are accelerating trains.

Coordinating the Operation of Trains

As shown in Figure 1, coordinating the operation of trains by overlapping accelerating and braking phases will influence the substation power requirement (*21*). Avoiding two trains accelerating at the same time can reduce the peak power, which can be realized by minimizing t_{aa}. Meanwhile, maximizing t_{ab} can reduce the substation energy consumption, where tractive energy consumption is partly provided by RBE. The t_{ab} is an indirect measure of the utilization rate of RBE (*18*), and the t_{aa} is an indirect measure of the duration of

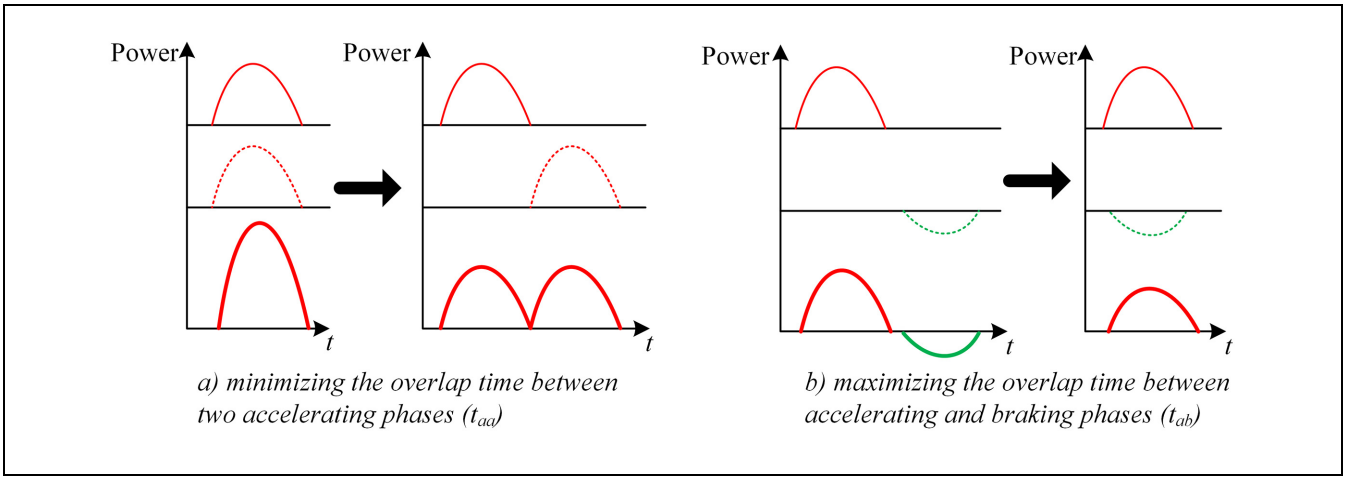

Figure 1. A sketch of train coordination.

substation peak power. To evaluate the energy-saving effect, some indicators are introduced as follows.

The total substation energy consumption can be calculated as:

$$E_{\text{sub}} = \int_{T_s}^{T_e} P_{\text{sub}}^{+}(t)dt \tag{1}$$

where

$$P_{\text{sub}}(t) = \sum_{n=1}^{K} P_n(t) \tag{2}$$

$$P_{\text{sub}}^{+}(t) = \begin{cases} P_{\text{sub}}(t) & P_{\text{sub}}(t) \geqslant 0 \\ 0 & P_{\text{sub}}(t) < 0 \end{cases} \tag{3}$$

$$P_{\text{sub}}^{-}(t) = \begin{cases} 0 & P_{\text{sub}}(t) \geqslant 0 \\ P_{\text{sub}}(t) & P_{\text{sub}}(t) < 0 \end{cases} \tag{4}$$

The total unutilized RBE can be calculated as:

$$E_{\text{urbe}} = \int_{T_s}^{T_e} P_{\text{sub}}^{-}(t)dt \tag{5}$$

and, the total available RBE can be calculated as:

$$E_{\text{arbe}} = \sum_{n=1}^{N} \left(\int_{T_s}^{T_e} P_n^{-}(t) \right) \tag{6}$$

where

$$P_n^{-} = \begin{cases} 0 & P_n(t) \geqslant 0 \\ P_n(t) & P_n(t) < 0 \end{cases} \tag{7}$$

and, the utilization rate of RBE can be calculated as:

$$\eta = 1 - E_{\text{urbe}}/E_{\text{arbe}} \tag{8}$$

The substation peak power can be calculated as:

$$P_p = \max(P_{\text{sub}}(t)) \tag{9}$$

Method

The Calculation of Overlap Times

As shown in Figure 2, in the running process of different directions (up and down) there are two types of overlap time: overlap time between accelerating phases (t_{aa}) and overlap time between accelerating and braking phases (t_{ab}). The departure and arrival times of trains determine the relative time position between the accelerating phases and the braking phases, which affects the calculation of overlap times. The calculation of overlap times is discussed in this section, in which train m and train n are taken as an example to illustrate the complex cases. The descriptions of the different cases of train coincidence are based on Ramos et al. (*16*).

Overlap Time between Accelerating Phases. According to the relationship between departure times of train m and train n, the calculation of t_{aa} can be divided into six cases as shown in Figure 3.

Case A1: condition as

$$D_{n,j} + t_{a,n,j} \leqslant D_{m,i} \tag{10}$$

then, t_{aa} can be calculated as

$$t_{aa} = 0 \tag{11}$$

Case A2: condition as

$$\begin{cases} D_{n,j} \leqslant D_{m,i} \\ D_{m,i} < D_{n,j} + t_{a,n,j} \leqslant D_{m,i} + t_{a,m,i} \end{cases} \tag{12}$$

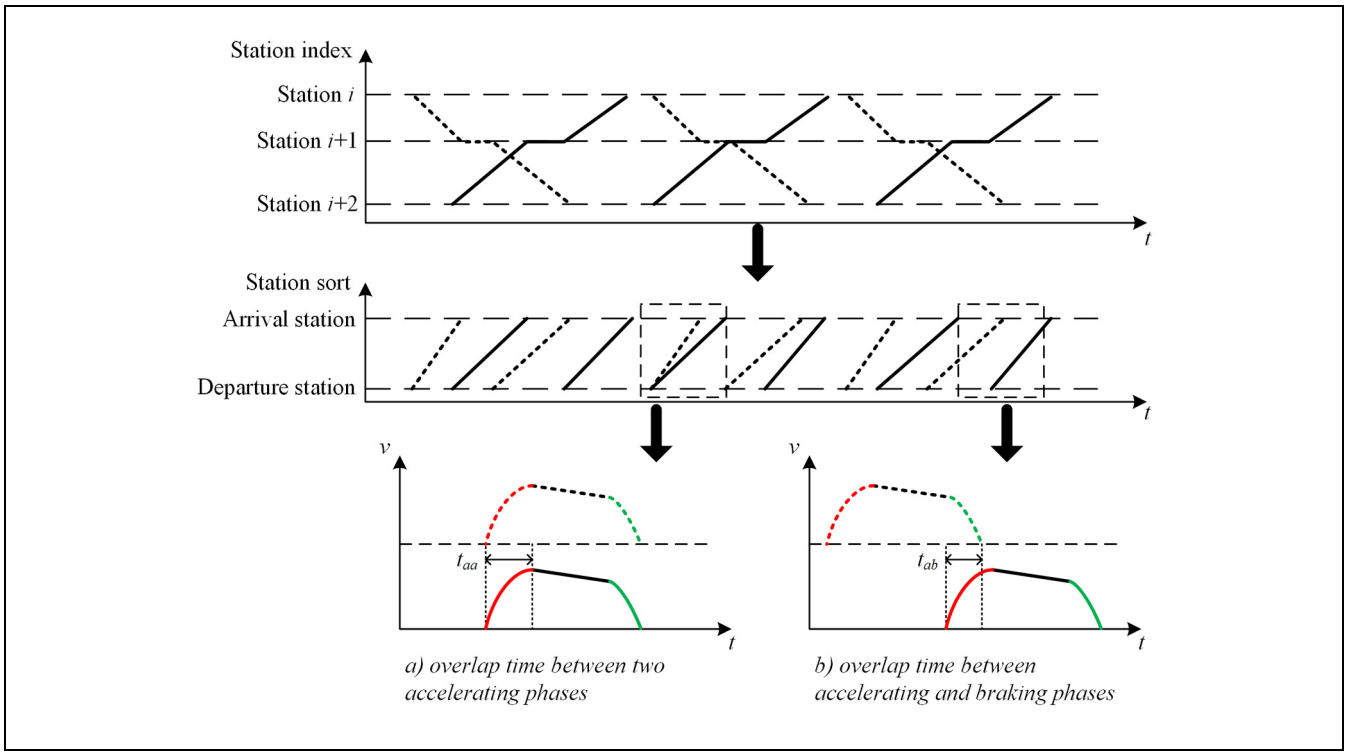

Figure 2. Two types of overlap times.

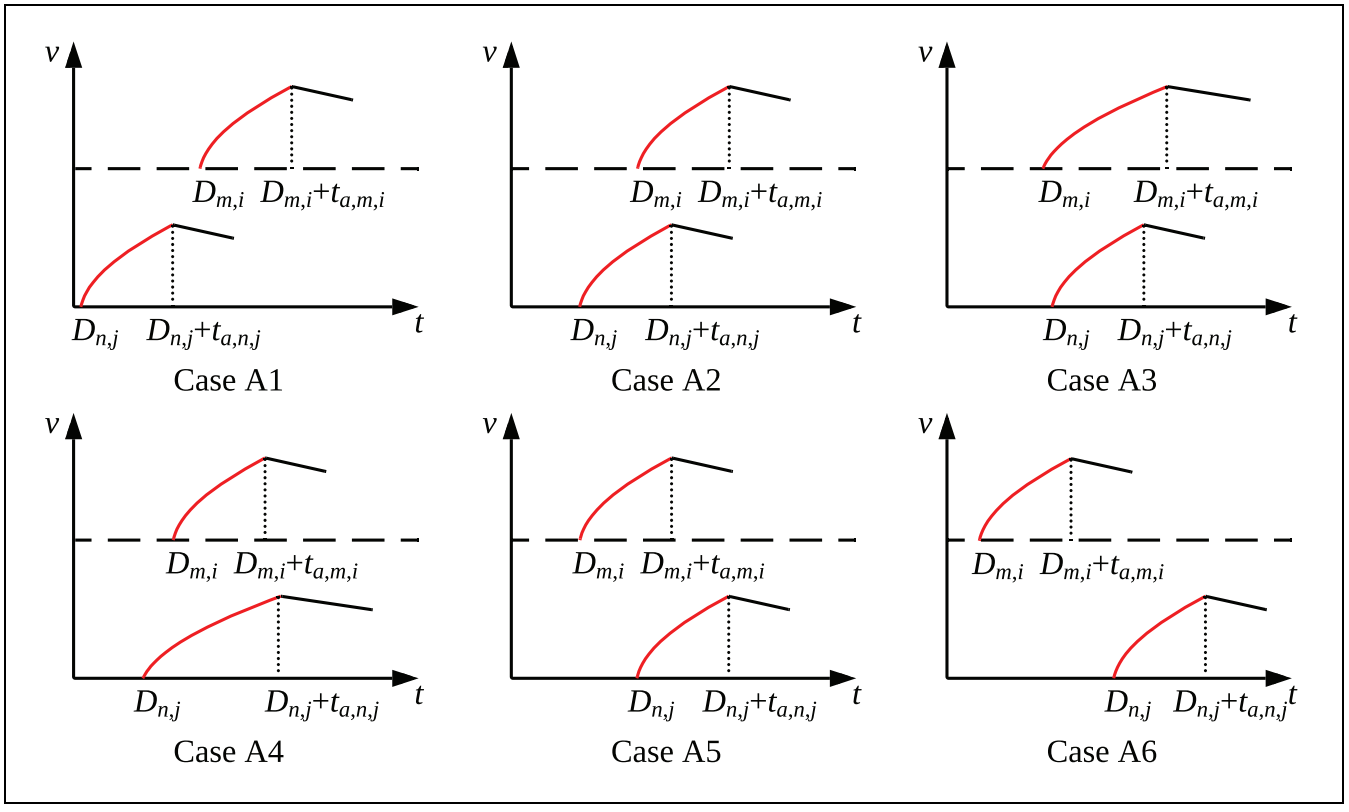

Figure 3. A sketch of six cases of the overlap time between accelerating phases (t_{aa}).

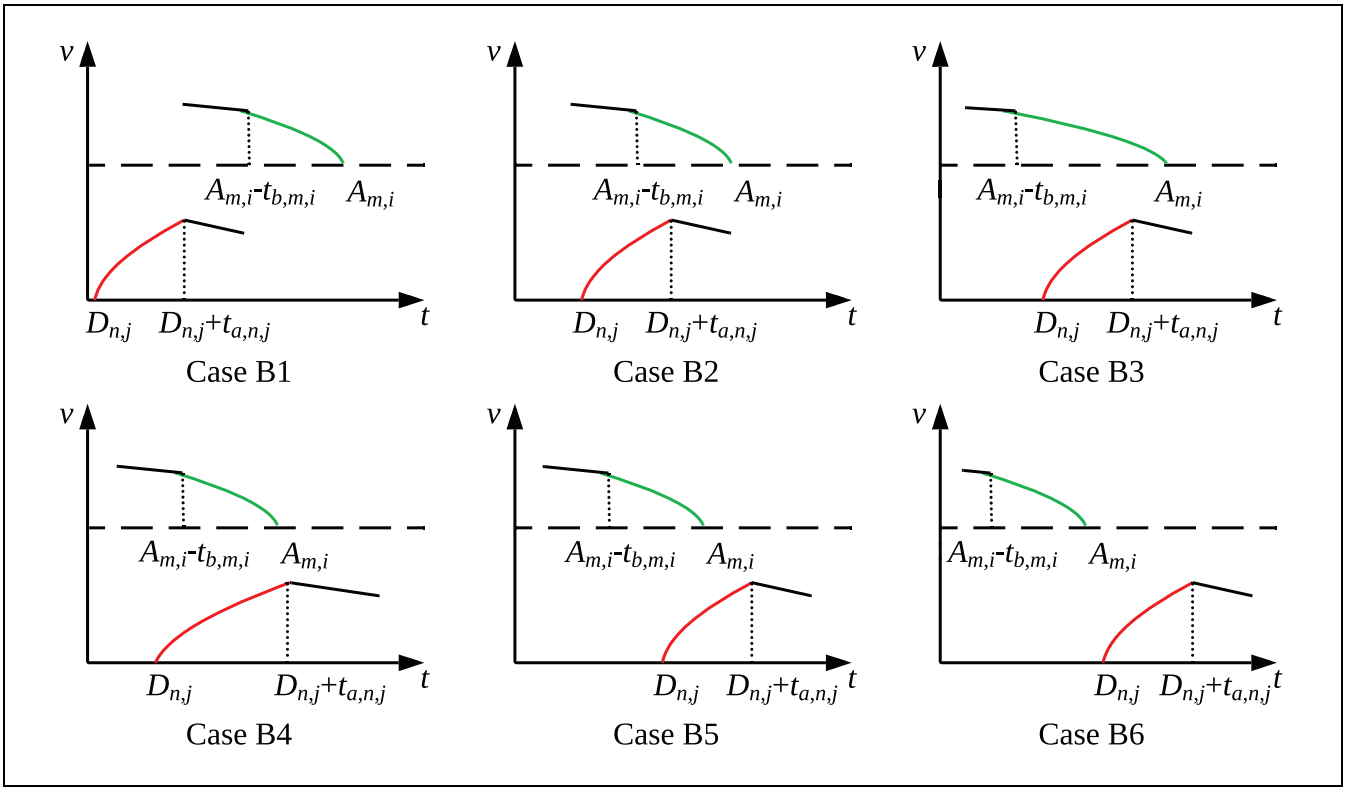

Figure 4. A sketch of six cases of the overlap time between accelerating and braking phases (t_{ab}).

then, t_{aa} can be calculated as

$$t_{aa} = D_{n,j} + t_{a,n,j} - D_{m,i} \tag{13}$$

Case A3: condition as

$$\begin{cases} D_{m,i} < D_{n,j} \leqslant D_{m,i} + t_{a,m,i} \\ D_{m,i} < D_{n,j} + t_{a,n,j} \leqslant D_{m,i} + t_{a,m,i} \end{cases} \tag{14}$$

then, t_{aa} can be calculated as

$$t_{aa} = t_{a,n,j} \tag{15}$$

Case A4: condition as

$$\begin{cases} D_{n,j} \leqslant D_{m,i} \\ D_{m,i} + t_{a,m,i} < D_{n,j} + t_{a,n,j} \end{cases} \tag{16}$$

then, t_{aa} can be calculated as

$$t_{aa} = t_{a,m,i} \tag{17}$$

Case A5: condition as

$$\begin{cases} D_{m,i} < D_{n,j} \leqslant D_{m,i} + t_{a,m,i} \\ D_{m,i} + t_{a,m,i} < D_{n,j} + t_{a,n,j} \end{cases} \tag{18}$$

then, t_{aa} can be calculated as

$$t_{aa} = D_{m,i} + t_{a,m,i} - D_{n,j} \tag{19}$$

Case A6: condition as

$$D_{m,i} + t_{a,m,i} < D_{n,j} \tag{20}$$

then, t_{aa} can be calculated as

$$t_{aa} = 0 \tag{21}$$

According to the above analysis of six cases, the calculation of t_{aa} of train m running in section $[i, i + 1]$ and train n running in section $[j, j + 1]$ can be described as

$$t_{aa}^{m,i,n,j} = f_{aa}\left(D_{m,i}, D_{n,j}, t_{a,m,i}, t_{a,n,j}\right) \tag{22}$$

Overlap Time Between Accelerating and Braking Phases. Similarly, according to the relationship between the arrival time of train m and the departure time of train n, the calculation of t_{ab} can be divided into six cases as shown in Figure 4.

Case B1: condition as

$$D_{n,j} + t_{a,n,j} \leqslant A_{m,i} - t_{b,m,i} \tag{23}$$

then, t_{ab} can be calculated as

$$t_{ab} = 0 \tag{24}$$

Case B2: condition as

$$\begin{cases} D_{n,j} \leqslant A_{m,i} - t_{b,m,i} \\ A_{m,i} - t_{b,m,i} < D_{n,j} + t_{a,n,j} \leqslant A_{m,i} \end{cases} \tag{25}$$

then, t_{ab} can be calculated as

$$t_{ab} = D_{n,j} + t_{a,n,j} - (A_{m,i} - t_{b,m,i}) \tag{26}$$

Case B3: condition as

$$\begin{cases} A_{m,i} - t_{b,m,i} < D_{n,j} \leqslant A_{m,i} \\ A_{m,i} - t_{b,m,i} < D_{n,j} + t_{a,n,j} \leqslant A_{m,i} \end{cases} \tag{27}$$

then, t_{ab} can be calculated as

$$t_{ab} = t_{a,n,j} \tag{28}$$

Case B4: condition as

$$\begin{cases} D_{n,j} \leqslant A_{m,i} - t_{b,m,i} \\ A_{m,i} < D_{n,j} + t_{a,n,j} \end{cases} \tag{29}$$

then, t_{ab} can be calculated as

$$t_{ab} = t_{b,m,i} \tag{30}$$

Case B5: condition as

$$\begin{cases} A_{m,i} - t_{b,m,i} < D_{n,j} \leqslant A_{m,i} \\ A_{m,i} < D_{n,j} + t_{a,n,j} \end{cases} \tag{31}$$

then, t_{ab} can be calculated as

$$t_{ab} = A_{m,i} - D_{n,j} \tag{32}$$

Case B6: condition as

$$A_{m,i} < D_{n,j} \tag{33}$$

then, t_{ab} can be calculated as

$$t_{ab} = 0 \tag{34}$$

According to the above analysis of six cases, the calculation of t_{ab} of train m running in section $[i,\ i+1]$ and train n running in section $[j,\ j+1]$ can be described as

$$t_{ab}^{m,i,n,j} = f_{ab}\left(A_{m,i}, D_{n,j}, t_{b,m,i}, t_{a,n,j}\right) \tag{35}$$

Model

Timetable Optimization Model. To improve the utilization of RBE and reduce the peak power, a timetable optimization model is built to maximize t_{ab} and minimize t_{aa}. The objective function can be described as

$$\min \sum_{m=1}^{N} \sum_{n=1}^{N} \sum_{i=1}^{2K-1} \sum_{j=1}^{2K-1} \left(w_{aa}\lambda_{aa}t_{aa}^{m,i,n,j} - w_{ab}\lambda_{ab}t_{ab}^{m,i,n,j}\right) \quad m \neq n \tag{36}$$

and the optimization model is subject to the following constraints:

(1) the constraint of runtimes

$$\begin{cases} A_{m,i} - D_{m,i} = R_{m,i} \\ A_{n,j} - D_{n,j} = R_{n,j} \end{cases} \tag{37}$$

(2) the constraint of departure times

$$\begin{cases} D_{m,i,\,\min} \leqslant D_{m,i} \leqslant D_{m,i,\,\max} \\ D_{n,j,\,\min} \leqslant D_{n,j} \leqslant D_{n,j,\,\max} \end{cases} \tag{38}$$

(3) the constraint of arrival times

$$\begin{cases} A_{m,i,\,\min} \leqslant A_{m,i} \leqslant A_{m,i,\,\max} \\ A_{n,j,\,\min} \leqslant A_{n,j} \leqslant A_{n,j,\,\max} \end{cases} \tag{39}$$

(4) the constraint of dwell times

$$\begin{cases} W_{m,i,\,\min} \leqslant D_{m,i} - A_{m,i} \leqslant W_{m,i,\,\max} \\ W_{n,j,\,\min} \leqslant D_{n,j} - A_{n,j} \leqslant W_{n,j,\,\max} \end{cases} \tag{40}$$

(5) the constraint of minimum safe headway

$$\begin{cases} D_{m+1,i} - D_{m,i} \geqslant T_s \\ A_{m+1,i} - A_{m,i} \geqslant T_s \\ D_{n+1,j} - D_{n,j} \geqslant T_s \\ A_{n+1,j} - A_{n,j} \geqslant T_s \end{cases} \tag{41}$$

MILP Model. To convert the timetable optimization model into a MILP model, logical and auxiliary variables are introduced to transform the objective function (36) into a linear equation, in which Equations 22 and 35 should be linearized. First, the linearization process of Equation 22 is introduced as follows.

Binary logical variables δ are introduced to distinguish the relationship between departure times of train m and train n, defined as

$$\left[D_{m,i} \leqslant D_{n,j}\right] \Leftrightarrow \left[\delta_1^{m,i,n,j} = 1\right] \tag{42}$$

$$\left[D_{n,j} + t_{a,n,j} \leqslant D_{m,i} + t_{a,m,i}\right] \Leftrightarrow \left[\delta_2^{m,i,n,j} = 1\right] \tag{43}$$

$$\left[D_{m,i} \leqslant D_{n,j} + t_{a,n,j}\right] \Leftrightarrow \left[\delta_3^{m,i,n,j} = 1\right] \tag{44}$$

$$\left[D_{n,j} \leqslant D_{m,i} + t_{a,m,i}\right] \Leftrightarrow \left[\delta_4^{m,i,n,j} = 1\right] \tag{45}$$

The definition (42) is equivalent to

$$\begin{cases} (D_{m,i} - t_{\max})\delta_1^{m,i,n,j} + D_{n,j} \leqslant D_{m,i} - \varepsilon \\ (D_{m,i} - t_{\min})\delta_1^{m,i,n,j} - D_{n,j} \leqslant -t_{\min} \end{cases} \tag{46}$$

where ε is a small positive number (typically the machine precision) that is introduced to transform strict inequality into non-strict inequality, which fits the MILP frameworks (*22*). The three other binary logical variables can be described in the same way. However, there is the product of the decision variable and the logical variable that does not fit the MILP framework. Thus, an auxiliary variable α is introduced to replace the product, defined as

$$\alpha_1^{m,i,n,j} = \delta_1^{m,i,n,j} D_{m,i} \tag{47}$$

The definition (47) is equivalent to

$$\begin{cases} \alpha_1^{m,i,n,j} \leqslant t_{\max}\delta_1^{m,i,n,j} \\ \alpha_1^{m,i,n,j} \geqslant t_{\min}\delta_1^{m,i,n,j} \\ \alpha_1^{m,i,n,j} \leqslant D_{m,i} - t_{\min}\left(1 - \delta_1^{m,i,n,j}\right) \\ \alpha_1^{m,i,n,j} \geqslant D_{m,i} - t_{\max}\left(1 - \delta_1^{m,i,n,j}\right) \end{cases} \tag{48}$$

Then, Equation 46 can be described as

$$\begin{cases} \alpha_1^{m,i,n,j} - t_{\max}\delta_1^{m,i,n,j} + D_{n,j} - D_{m,i} \leqslant -\varepsilon \\ \alpha_1^{m,i,n,j} - t_{\min}\delta_1^{m,i,m,j} - D_{n,j} \leqslant -t_{\min} \end{cases} \tag{49}$$

Similarly, the three other auxiliary variables are introduced to replace the products of decision variables and logical variables, defined as

$$\begin{aligned} \alpha_2^{m,i,n,j} = \delta_2^{m,i,n,j} D_{m,i}, \alpha_3^{m,i,n,j} = \delta_3^{m,i,n,j} D_{m,i}, \\ \alpha_4^{m,i,n,j} = \delta_4^{m,i,n,j} D_{m,i} \end{aligned} \tag{50}$$

These three auxiliary variables can be described in the same way as Equation 48. With the help of logical variables, the calculation formula (22) for t_{aa} can be rewritten as

$$\begin{aligned} t_{aa}^{m,i,n,j} = \delta_3^{m,i,n,j}\delta_4^{m,i,n,j}[&\left(1 - \delta_1^{m,i,n,j}\right)\delta_2^{m,i,n,j} \\ &\left(D_{n,j} + t_{a,n,j} - D_{m,i}\right) + \delta_1^{m,i,n,j}\delta_2^{m,i,n,j} t_{a,n,j} \\ &+ \left(1 - \delta_1^{m,i,n,j}\right)\left(1 - \delta_2^{m,i,n,j}\right) t_{a,m,i} + \delta_1^{m,i,n,j} \\ &\left(1 - \delta_2^{m,i,n,j}\right)\left(D_{m,i} + t_{a,m,i} - D_{n,j}\right)] \end{aligned} \tag{51}$$

The products of the two logical variables in Equation 51 also do not fit the MILP framework. Logical variables are introduced, therefore, to replace these products, defined as

$$\delta_5^{m,i,n,j} = \delta_3^{m,i,n,j}\delta_4^{m,i,n,j} \tag{52}$$

and this binary logical variable is equivalent to

$$\begin{cases} -\delta_3^{m,i,n,j} + \delta_5^{m,i,n,j} \leqslant 0 \\ -\delta_4^{m,i,n,j} + \delta_5^{m,i,n,j} \leqslant 0 \\ \delta_3^{m,i,n,j} + \delta_4^{m,i,n,j} - \delta_5^{m,i,n,j} \leqslant 1 \end{cases} \tag{53}$$

Similarly, another two logical variables are defined as

$$\delta_6^{m,i,n,j} = \delta_1^{m,i,n,j}\,\delta_5^{m,i,n,j}, \delta_7^{m,i,n,j} = \delta_2^{m,i,n,j}\delta_5^{m,i,n,j} \tag{54}$$

which can be described in the same way as Equation 53. Then, Equation 51 can be rewritten as

$$\begin{aligned} t_{aa}^{m,i,n,j} = \delta_5^{m,i,n,j} t_{a,i} + \delta_6^{m,i,n,j}\left(D_{m,i} - D_{n,j}\right) + \delta_7^{m,i,n,j} \\ \left(D_{n,j} + t_{a,j} - D_{m,i} - t_{a,i}\right) \end{aligned} \tag{55}$$

The products of logical variables and decision variables in Equation 55 again do not fit the MILP framework. Auxiliary variables are introduced to replace these products, defined as

$$\begin{aligned} \alpha_5^{m,i,n,j} = \delta_6^{m,i,n,j} D_{n,j}, \alpha_6^{m,i,n,j} = \delta_7^{m,i,n,j} D_{n,j}, \alpha_7^{m,i,n,j} = \\ \delta_6^{m,i,n,j} D_{m,i}, \alpha_8^{m,i,n,j} = \delta_7^{m,i,n,j} D_{m,i} \end{aligned} \tag{56}$$

and these auxiliary variables can be described in the same way as Equation 48. Then, Equation 55 can be rewritten as

$$\begin{aligned} t_{aa}^{m,i,n,j} &= t_{a,m,i}\delta_5^{m,i,n,j} + \left(t_{a,n,j} - t_{a,m,i}\right)\delta_7^{m,i,n,j} \\ &\quad - \alpha_5^{m,i,n,j} + \alpha_6^{m,i,n,j} + \alpha_7^{m,i,n,j} - \alpha_8^{m,i,n,j} \\ &= f_{aa}\left(D_{m,i}, D_{n,j}, t_{a,m,i}, t_{a,n,j}, \boldsymbol{\delta}^{m,i,n,j}, \boldsymbol{\alpha}^{m,i,n,j}\right) \end{aligned} \tag{57}$$

where

$$\begin{aligned} &\boldsymbol{\delta}^{m,i,n,j} = \\ &\left[\delta_1^{m,i,n,j}, \delta_2^{m,i,n,j}, \delta_3^{m,i,n,j}, \delta_4^{m,i,n,j}, \delta_5^{m,i,n,j}, \delta_6^{m,i,n,j}, \delta_7^{m,i,n,j}\right] \\ &\boldsymbol{\alpha}^{m,i,n,j} = \\ &\left[\alpha_1^{m,i,n,j}, \alpha_2^{m,i,n,j}, \alpha_3^{m,i,n,j}, \alpha_4^{m,i,n,j}, \alpha_5^{m,i,n,j}, \alpha_6^{m,i,n,j}, \alpha_7^{m,i,n,j}, \alpha_8^{m,i,n,j}\right] \end{aligned} \tag{58}$$

With the help of logical and auxiliary variables, the calculation formula about t_{aa} is transformed into a linear function (57), which fits the MILP framework. Similarly, logical and auxiliary variables are introduced to linearize Equation 35. Binary logical variables η are introduced to distinguish the relationship between the arrival time of train m and the departure time of train n, which are defined as

$$\begin{aligned} &\left[A_{m,i} - t_{b,m,i} \leqslant D_{n,j}\right] \Leftrightarrow \left[\eta_1^{m,i,n,j} = 1\right] \\ &\left[D_{n,j} + t_{a,n,j} \leqslant A_{m,i}\right] \Leftrightarrow \left[\eta_2^{m,i,n,j} = 1\right] \\ &\left[A_{m,i} - t_{b,m,i} \leqslant D_{n,j} + t_{a,n,j}\right] \Leftrightarrow \left[\eta_3^{m,i,n,j} = 1\right] \\ &\left[D_{n,j} \leqslant A_{m,i}\right] \Leftrightarrow \left[\eta_4^{m,i,n,j} = 1\right] \end{aligned} \tag{59}$$

which are equivalent to the function like Equation 46. Meanwhile, other binary logical variables are introduced to replace the products of two binary logical variables, defined as

$$\eta_5^{m,i,n,j} = \eta_3^{m,i,n,j}\eta_4^{m,i,n,j}, \eta_6^{m,i,n,j} = \eta_1^{m,i,n,j}\eta_5^{m,i,n,j}, \quad \eta_7^{m,i,n,j} = \eta_2^{m,i,n,j}\eta_5^{m,i,n,j} \tag{60}$$

These binary logical variables can be defined in the same way as Equation 52. Auxiliary variables are introduced to replace the products of logical variables and decision variables, defined as

$$\begin{aligned} &\beta_1^{m,i,n,j} = \eta_1^{m,i,n,j}A_{m,i}, \beta_2^{m,i,n,j} = \eta_2^{m,i,n,j}A_{m,i}, \\ &\beta_3^{m,i,n,j} = \eta_3^{m,i,n,j}A_{m,i}, \beta_4^{m,i,n,j} = \eta_4^{m,i,n,j}A_{m,i}, \\ &\beta_5^{m,i,n,j} = \eta_6^{m,i,n,j}D_{n,j}, \beta_6^{m,i,n,j} = \eta_7^{m,i,n,j}D_{n,j}, \\ &\beta_7^{m,i,n,j} = \eta_6^{m,i,n,j}A_{m,i}, \beta_8^{m,i,n,j} = \eta_7^{m,i,n,j}A_{m,i} \end{aligned} \tag{61}$$

These auxiliary logical variables can be defined in the same way as Equation 48. Then, Equation 35 can be rewritten as

$$\begin{aligned} t_{ab}^{m,i,n,j} &= t_{b,m,i}\eta_5^{m,i,n,j} - t_{b,m,i}\eta_6^{m,i,n,j} + t_{a,n,j}\eta_7^{m,i,n,j} \\ &\quad - \beta_5^{m,i,n,j} + \beta_6^{m,i,n,j} + \beta_7^{m,i,n,j} - \beta_8^{m,i,n,j} \\ &= f_{ab}\left(A_{m,i}, D_{n,j}, t_{b,m,i}, t_{a,n,j}, \boldsymbol{\eta}^{m,i,n,j}, \boldsymbol{\beta}^{m,i,n,j}\right) \end{aligned} \tag{62}$$

where

$$\begin{aligned} &\boldsymbol{\eta}^{m,i,n,j} = \\ &\left[\eta_1^{m,i,n,j}, \eta_2^{m,i,n,j}, \eta_3^{m,i,n,j}, \eta_4^{m,i,n,j}, \eta_5^{m,i,n,j}, \eta_6^{m,i,n,j}, \eta_7^{m,i,n,j}\right] \\ &\boldsymbol{\beta}^{m,i,n,j} = \\ &\left[\beta_1^{m,i,n,j}, \beta_2^{m,i,n,j}, \beta_3^{m,i,n,j}, \beta_4^{m,i,n,j}, \beta_5^{m,i,n,j}, \beta_6^{m,i,n,j}, \beta_7^{m,i,n,j}, \beta_8^{m,i,n,j}\right] \end{aligned} \tag{63}$$

After the transformation, the timetable optimization model can be described as a MILP model. Decision variables of the MILP model are defined as

$$\mathbf{X} = [\mathbf{D}, \mathbf{A}, \boldsymbol{\delta}, \boldsymbol{\alpha}, \boldsymbol{\eta}, \boldsymbol{\beta}]^T \tag{64}$$

where the matrix $\boldsymbol{D}$ can be described as

$$\begin{aligned} \mathbf{D} = [&D_{1,1}, D_{1,2} \cdots D_{1,2K}, D_{2,1}, D_{22} \cdots \\ &D_{2,2K} \cdots\cdots D_{N,1}D_{N,2} \cdots D_{N,2K}] \end{aligned} \tag{65}$$

Similarly, the matrix $\boldsymbol{A}$, $\boldsymbol{\delta}$, $\boldsymbol{\alpha}$, $\boldsymbol{\eta}$ and $\boldsymbol{\beta}$ can be described in the same way. Then, the MILP model can be formulated as

$$\min \mathbf{FX} \tag{66}$$

subject to

$$\mathbf{M}_1\mathbf{X} \leqslant \mathbf{m}_1 \tag{67}$$

$$\mathbf{M}_2\mathbf{X} = \mathbf{m}_2 \tag{68}$$

where $\boldsymbol{F}$ can be defined according to Equations 57 and 62, $\boldsymbol{M}_1$ and $\boldsymbol{m}_1$ can be defined according to the constraints (38–41) and the definition of binary logical and auxiliary variables (48), (49) and (53). $\boldsymbol{M}_2$ and $\boldsymbol{m}_2$ can be defined according to Equation 37. The MILP problem can be solved by branch-and-bound algorithms implemented in several existing commercial and free solvers. In this paper, CPLEX Solver is used to solve the MILP problem.

Simulations

Simulation Conditions

To verify the performance of the proposed method, simulations are presented based on the data from one of Guangzhou Metro Lines. The metro line consists of 15 stations and seven substations. The service time is from 5:30 to 22:30, and the headway for all-day operation mainly includes three types: 180 s, 270 s, and 360 s. Considering the dimensions of t_{aa} and t_{ab} are the same, the weight parameters w_{aa} and w_{ab} are both set to be 1. Substation power data of trains come from a single train running simulator. The maximum train power is about 15 MW, then we define substation power over 16 MW as substation peak power. Three optimal timetables with different influence factors are compared with the original timetable, stating as:

- **original timetable:** timetable which is based on the pre-given setting;
- **optimal timetable ($\boldsymbol{\lambda_{aa} = 1, \lambda_{ab} = 0}$):** optimal timetable which only considers minimizing t_{aa};
- **optimal timetable ($\boldsymbol{\lambda_{aa} = 0, \lambda_{ab} = 1}$):** optimal timetable which only considers maximizing t_{ab};
- **optimal timetable ($\boldsymbol{\lambda_{aa} = 1, \lambda_{ab} = 1}$):** optimal timetable which considers minimizing t_{aa} as well as maximizing t_{ab}.

Simulation for All-Day Operation

The performances of the four timetables for all-day operation are shown in Table 2. Comparing the original timetable with the three optimal timetables, the overlap times have been changed dramatically by adjusting the timetable. Especially, t_{ab} varies from 28,630 s of the original timetable up to 76,251 s of the optimal timetable ($\lambda_{aa} = 0$, $\lambda_{ab} = 1$), and t_{aa} varies from 12,816 s of the original timetable down to 2,584 s of the optimal timetable ($\lambda_{aa} = 1$, $\lambda_{ab} = 0$). In addition, changes in the overlap

Table 2. Performances of Four Timetables for All-Day Operation

Index	Original timetable	Optimal timetable ($\lambda_{aa} = 1, \lambda_{ab} = 0$)	Optimal timetable ($\lambda_{aa} = 0, \lambda_{ab} = 1$)	Optimal timetable ($\lambda_{aa} = 1, \lambda_{ab} = 1$)
Overlap time between accelerating and braking phases (t_{ab}) (s)	28,630	23,993	76,251	72,683
Overlap time between accelerating phases (t_{aa}) (s)	12,816	2,584	14,684	7,056
Energy consumption (kWh)	486,554	477,535	422,191	417,299
Rate of energy saving (%)	NA	2	13	14
Utilization rate of RBE (%)	27	30	48	50
Duration of substation power over 16 MW (s)	11,730	3,568	11,594	3,984

Note: RBE = regenerative braking energy; NA = not available.

Table 3. Performances of Four Timetables during Peak Hours (7:00–8:00)

Index	Original timetable	Optimal timetable ($\lambda_{aa} = 1, \lambda_{ab} = 0$)	Optimal timetable ($\lambda_{aa} = 0, \lambda_{ab} = 1$)	Optimal timetable ($\lambda_{aa} = 1, \lambda_{ab} = 1$)
Overlap time between accelerating and braking phases (t_{ab}) (s)	1,693	1,537	4,566	4,120
Overlap time between accelerating phases (t_{aa}) (s)	1,543	323	1,798	882
Energy consumption (kWh)	34,103	32,122	30,107	29,496
Rate of energy saving (%)	NA	13	27	30
Utilization rate of RBE (%)	31	40	49	52
Duration of substation power over 16 MW (s)	1,425	446	1,423	498

Note: RBE = regenerative braking energy; NA = not available.

times have a huge impact on the substation power. The utilization rate of RBE varies from 27% of the original timetable to 30%, 48%, and 50% of the optimal timetable ($\lambda_{aa} = 1$, $\lambda_{ab} = 0$), the optimal timetable ($\lambda_{aa} = 0$, $\lambda_{ab} = 1$), and the optimal timetable ($\lambda_{aa} = 1$, $\lambda_{ab} = 1$), respectively. Compared with the original timetable, the substation energy consumption of the three optimal timetables is reduced by 2%, 13%, and 14%, respectively. Meanwhile, the duration of substation power over 16 MW varies from 11,730 s of the original timetable to 3,568 s, 11,594 s, and 3,984 s of the optimal timetable (λaa = 1, λab = 0), the optimal timetable (λaa = 0, λab = 1), and the optimal timetable (λaa = 1, λab = 1), respectively. Compared with the original timetable, the duration of substation power over 16 MW of the three optimal timetables is reduced by 70%, 1%, and 66%, respectively. From the all-day operation simulation results, the advantage of minimizing t_{aa} is mainly to reduce the duration of substation peak power, but it is limited to improve the utilization of RBE by minimizing t_{aa}. On the other hand, improving the utilization of RBE can be achieved by maximizing t_{ab}. The optimal timetable ($\lambda_{aa} = 1$, $\lambda_{ab} = 1$) combining minimizing t_{aa} and maximizing t_{ab} achieves good performance in both aspects.

Simulation for Peak and Off-Peak Hours

The performances of four timetables during peak hours (7:00–8:00) and off-peak hours (14:00–15:00) are shown in Tables 3 and 4, respectively. The headway during peak hours (7:00–8:00) is 180 s, and the headway during off-peak hours (14:00–15:00) is 360 s. During the peak hours, the utilization rate of RBE of the original timetable is already at a high level (31%); it can still be improved to 40%, 49%, and 52%, respectively, by applying the proposed methods. Meanwhile, compared with the original timetable, the duration of substation power over 16 MW of the three optimal timetables is reduced by 69%, 0.1%, and 65%, respectively. It is almost impossible to reduce the duration of substation peak power by maximizing t_{ab}. During the off-peak hours, the t_{aa} is already at a small value (40 s), and the beneficial effects brought by minimizing t_{aa} are limited. Only the duration of substation peak power is reduced from 28 s of the original timetable to 17 s of the optimal timetable ($\lambda_{aa} = 1$, $\lambda_{ab} = 0$). Comparing the original timetable with the optimal timetable ($\lambda_{aa} = 1$, $\lambda_{ab} = 0$), the utilization rate of RBE drops from 17% to 12%, and the energy consumption rises from 18,553 kWh to 19,086 kWh. On the other hand, the optimal timetable ($\lambda_{aa} = 0$, $\lambda_{ab} = 1$) and the

Table 4. Performances of Four Timetables During Off-Peak Hours (14:00–15:00)

Index	Original timetable	Optimal timetable ($\lambda_{aa} = 1, \lambda_{ab} = 0$)	Optimal timetable ($\lambda_{aa} = 0, \lambda_{ab} = 1$)	Optimal timetable ($\lambda_{aa} = 1, \lambda_{ab} = 1$)
Overlap time between accelerating and braking phases (t_{ab}) (s)	970	812	3,030	3,030
Overlap time between accelerating phases (t_{aa}) (s)	40	0	24	0
Energy consumption (kWh)	18,553	19,086	15,982	15,982
Rate of energy saving (%)	NA	−2	14	14
Utilization rate of RBE (%)	17	12	41	41
Duration of substation power over 16 MW (s)	28	0	17	0

Note: RBE = regenerative braking energy; NA = not available.

optimal timetable ($\lambda_{aa} = 1, \lambda_{ab} = 1$) still have significant advantages in energy saving.

The optimal timetable ($\lambda_{aa} = 1, \lambda_{ab} = 0$) only focuses on minimizing t_{aa}, where t_{aa} and the duration of substation peak power are reduced to smaller values. Although trains are coordinated to avoid accelerating at the same time, the RBE is not fully utilized without overlapping accelerating and braking phases. The optimal timetable ($\lambda_{aa} = 0, \lambda_{ab} = 1$) is better than the optimal timetable ($\lambda_{aa} = 1, \lambda_{ab} = 0$) in improving the utilization of RBE, which indicates that the method of maximizing t_{ab} is a better way to reduce energy consumption. Comparing the three optimal timetables, the timetable optimization method that involves minimizing t_{aa} and maximizing t_{ab} is the best way to improve the energy-efficient effect and reduce the substation peak power. It has been shown, therefore, that minimizing t_{aa} can reduce the duration of substation peak power more significantly and maximizing t_{ab} can improve the utilization of RBE more effectively. In addition, combining minimizing t_{aa} and maximizing t_{ab} has significant effects both in improving the utilization of RBE and reducing the substation peak power.

Discussion

The simulation results show that the duration of substation peak power can be reduced by minimizing t_{aa} and the utilization of RBE can be improved by maximizing t_{ab}. The timetable optimization model was transformed into a MILP model by linearizing the calculation of the overlap times, which makes the model simpler compared with the models of other studies (*16–19*). In addition, the MILP model can be solved to achieve the optimal solution. The overlap time between accelerating phases (t_{aa}) is introduced first in this paper, and is minimized to reduce the peak power. The simulation results show that the timetable optimization method combining minimizing t_{aa} and maximizing t_{ab} is more energy-efficient than the traditional method (*16–19*) that only considers maximizing t_{ab}. In the studies of energy-efficient train scheduling based on the overlap time, the objective goal of improving the utilization of RBE is simplified to minimize t_{ab}, and the simulation results show that the utilization of RBE can be improved by minimizing the overlap time. In addition, to improve the utilization more precisely and efficiently, the relationship between t_{ab} and the utilization of RBE should be researched in future work.

Conclusions

In this paper, we propose an energy-efficient train scheduling approach for metro transit systems. The overlap time between accelerating and braking phases (t_{ab}) is maximized to improve the utilization of RBE. Meanwhile, the overlap time between accelerating phases (t_{aa}) is minimized to reduce the substation peak power. Taking into account the timetable constraints, a timetable optimization model has been built to optimize the overlap times. With the help of logical and auxiliary variables, the optimization model was then transformed into a MILP model. In addition, simulations are presented to prove the feasibility of the approach. Thanks to the change in the overlap times, the utilization of RBE is improved and the duration of substation peak power is reduced. The adjustment of the departure and arrival times respects the constraints (37–41), which results in running times and dwell times within a reasonable range. Thus, the optimal timetable can be applied in practice. In the train scheduling phase, the energy-efficient timetable can be used by dispatchers to reduce operational costs. However, not only the operating costs but also the quality of service should be considered by dispatchers. In future work, passenger waiting time and timetable robustness should be considered to obtain a more efficient timetable. On the other hand, the timetable rescheduling problem should be researched in future work to maintain the good qualities of optimal timetables under disturbances.

Acknowledgment

The authors would like to thank the reviewers for their helpful comments and valuable suggestions which improved this paper substantially.

Author Contributions

The authors confirm contribution to the paper as follows: study conception and design: XF, BJ, QW, PS, QF; data collection: XF, BJ, QW, PS; analysis and interpretation of results: BJ, PS, QF; draft manuscript preparation: BJ, QW, PS, QF. All authors reviewed the results and approved the final version of the manuscript.

Declaration of Conflicting Interests

The author(s) declared no potential conflicts of interest with respect to the research, authorship, and/or publication of this article.

Funding

The author(s) disclosed receipt of the following financial support for the research, authorship, and/or publication of this article: This study has been funded by the project on the development of key technology and equipment for freight trains with a speed of 160 km/h (Grant No. 2017YFB1201302).

References

1. González-Gil, A., R. Palacin, P. Batty, and J. P. Powell. A Systems Approach to Reduce Urban Rail Energy Consumption. *Energy Conversion and Management*, Vol. 80, 2014, pp. 509–524.
2. González-Gil, A., R. Palacin, and P. Batty. Optimal Energy Management of Urban Rail Systems: Key Performance Indicators. *Energy Conversion and Management*, Vol. 90, 2015, pp. 282–291.
3. Yang, X., X. Li, B. Ning, and T. Tang. A Survey on Energy-Efficient Train Operation for Urban Rail Transit. *IEEE Transactions on Intelligent Transportation Systems*, Vol. 17, No. 1, 2016, pp. 2–13.
4. Scheepmaker, G. M., R. M. P. Goverde, and L. G. Kroon. Review of Energy-Efficient Train Control and Timetabling. *European Journal of Operational Research*, Vol. 257, No. 2, 2017, pp. 355–376.
5. Pudney, P. J., and P. G. Howlett. Optimal Driving Strategy for a Train Journey with Speed Limits. *The ANZIAM Journal*, Vol. 36, No. 1, 1994, pp. 38–49.
6. Howlett, P. G., and J. Cheng. Optimal Driving Strategies for a Train on a Track with Continuously Varying Gradient. *The ANZIAM Journal*, Vol. 38, No. 3, 1997, pp. 388–410.
7. Jin, B., P. Sun, M. Xu, and Q. Wang. Train Timetable and Trajectory Optimization using Improved State-Space MILP. *Proc., 37th Chinese Control Conference (CCC)*, IEEE, Wuhan, 2018, pp. 7748–7753.
8. González-Gil, A., R. Palacin, and P. Batty. Sustainable Urban Rail Systems: Strategies and Technologies for Optimal Management of Regenerative Braking Energy. *Energy Conversion and Management*, Vol. 75, 2013, pp. 374–388.
9. Rupp, A., H. Baier, P. Mertiny, and M. Secanell. Analysis of a Flywheel Energy Storage System for Light Rail Transit. *Energy*, Vol. 107, 2016, pp. 625–638.
10. Sun, X., H. Lu, and H. Dong. Energy-Efficient Train Control by Multi-Train Dynamic Cooperation. *IEEE Transactions on Intelligent Transportation Systems*, Vol. 18, No. 11, 2017, pp. 3114–3121.
11. Liu, J., H. Guo, and Y. Yu. Research on the Cooperative Train Control Strategy to Reduce Energy Consumption. *IEEE Transactions on Intelligent Transportation Systems*, Vol. 1, No. 5, 2016, pp. 1–9.
12. Su, S., T. Tang, and C. Roberts. A Cooperative Train Control Model for Energy Saving. *IEEE Transactions on Intelligent Transportation Systems*, Vol. 16, No. 2, 2015, pp. 622–631.
13. Liu, H., B. Ning, T. Tang, and X. Guo. Maximize Regenerative Energy Utilization Through Timetable Optimization in a Subway System. *Proc., 2018 International Conference on Intelligent Rail Transportation (ICIRT)*, IEEE, Singapore, 2018, pp. 1–5.
14. Wang, X., T. Tang, S. Su, X. Liu, and T. Ma. Energy-Efficient Operation of Multi-Trains for Metro Systems with Considering the Regenerative Energy. *Proc., 2018 International Conference on Intelligent Rail Transportation (ICIRT)*, IEEE, Singapore, 2018, pp. 1–5.
15. Albrecht, T. Reducing Peak Powers and Energy Consumption in Rail Transit Systems by Simultaneous Train Running Time Control. In *Computers in Railways IX*, WIT Press, Southampton, 2004, pp. 885–894.
16. Ramos, A., M. Pena, A. Fernández-Cardador, and A. P. Cucala. Mathematical Programming Approach to Underground Timetabling Problem for Maximizing Time Synchronization. *Proc., International Conference on Industrial Engineering, Management*, Madrid, 2007, pp. 88–95.
17. Yang, X., X. Li, Z. Gao, H. Wang, and T. Tang. A Cooperative Scheduling Model for Timetable Optimization in Subway Systems. *IEEE Transactions on Intelligent Transportation Systems*, Vol. 14, No. 1, 2013, pp. 438–447.
18. Ning, J., Y. Zhou, F. Long, and X. Tao. A Synergistic Energy-Efficient Planning Approach for Urban Rail Transit Operations. *Energy*, Vol. 151, 2018, pp. 854–863.
19. Zhao, L., K. Li, and S. Su. A Multi-Objective Timetable Optimization Model for Subway Systems. *Proc., 2013 International Conference on Electrical and Information Technologies for Rail Transportation (EITRT2013)*, Springer, Berlin, Heidelberg, Vol. 1, 2014, pp. 557–565.
20. Sanso, B., and P. Girard. Instantaneous Power Peak Reduction and Train Scheduling Desynchronization in Subway Systems. *Transportation Science*, Vol. 31, No. 4, 1997, pp. 312–323.
21. Kim, K. M., K. T. Kim, and M. S. Han. A Model and Approaches for Synchronized Energy Saving in Timetabling. *Proc., IEEE 9th World Congress on Railway Research*, Lille, 2011.
22. Bemporad, A., and M. Morari. Control of Systems Integrating Logic, Dynamics, and Constraints. *Automatica*, Vol. 35, No. 3, 1999, pp. 407–427.